

Decizie de indexare a faptei de plagiat la poziția 00385 / 03.07.2017 și pentru admitere la publicare în volum tipărit

care se bazează pe:

A. Nota de constatare și confirmare a indiciilor de plagiat prin fișa suspiciunii inclusă în decizie.

Fișa suspiciunii de plagiat / Sheet of plagiarism's suspicion	
Opera suspicionată (OS)	Opera autentică (OA)
Suspicious work	Authentic work
OS	Ioachim Andrei, Toacșan Mariana Irina, Banciu Marin Gabriel, Nedelcu Liviu, Dutu Constantin Augustin, Alexandru V. Horia, Antohe Stefan, Andronescu E, Jinga Sorin, Niță Petru. Synthesis and properties of Ba (Zn 1/3 Ta 2/3) O3 for microwave and millimeter wave applications. <i>Thin Solid Films</i> . 2008 Feb 15;516(7):1558-1562. Note: a) the source of suspicion: www.integru.org . b) This work was supported by Ministry of Education and Research under contract CEEX No. 4 / 2005. c) The papers was RETRACTED by the editor.
OA	Ioachim A, Toacșan M.I, Banciu M.G, Nedelcu L, Duțu C.A, Feder M, Plăpcianu C, Lifei F, and Niță P. Effect of the sintering temperature on the Ba (Zn 1/3 Ta 2/3) O3 dielectric properties. <i>Journal of the European Ceramic Society</i> . 2007 Dec 31;27(2):1117-1122. (Available on-line in 12 June 2006). Note: This work was supported by Ministry of Education and Research under contract nr: 09N/505.2003.
Incidența minimă a suspiciunii / Minimum incidence of suspicion	
p.1559:02s – p.1559: 35s	p.1117:10d – p.1118:23s
p.1559:37s – p.1559:08d	p.1118:26s – p.1118:35s
p.1559:Fig.2	p.1118:Fig.1
p.1559:09d – p.1560:14s	p.1118:37s – p.1118:25d
p.1560:19d – p.1560:31s	p.1119:21s – p.1119:32s
p.1560:04d – p.1560:14s	p.1119:33s – p.1119:45s
p.1560:21d – p.1561:03s	p.1119:34s – p.1119:03d
p.1561:10s – p.1561:21s	p.1120:08d – p.1120:19d
p.1561:22s – p.1561:23d	p.1120:21d – p.1120:44d
p.1561:Fig.7	p.1121:Fig.9
p.1561:Fig.6	p.1121:Fig.7
p.1562:34d – p.1561:38d; p.1562:10s – 1562:03d	p.1121:06d – p.1122:05s
Fișa întocmită pentru includerea suspiciunii în Indexul Operelor Plagiate în România de la Sheet drawn up for including the suspicion in the Index of Plagiarized Works in Romania at www.plagiate.ro	

Notă: Prin „p.72:00” se înțelege paragraful care se termină la finele pag.72. Notația „p.00:00” semnifică până la ultima pagină a capitolului curent, în întregime de la punctul inițial al preluării.

Note: By „p.72:00” one understands the text ending with the end of the page 72. By „p.00:00” one understands the taking over from the initial point till the last page of the current chapter, entirely.

B. Fișa de argumentare a calificării de plagiat alăturată, fișă care la rândul său este parte a deciziei.

Echipa Indexului Operelor Plagiate în România

Fișa de argumentare a calificării

Nr. crt.	Descrierea situației care este încadrată drept plagiat	Se confirmă
1.	Preluarea identică a unor pasaje (piese de creație de tip text) dintr-o operă autentică publicată, fără precizarea întinderii și menționarea provenienței și însușirea acestora într-o lucrare ulterioară celei autentice.	✓
2.	Preluarea a unor pasaje (piese de creație de tip text) rezumate dintr-o operă autentică publicată, fără precizarea întinderii și menționarea provenienței și însușirea acestora într-o lucrare ulterioară celei autentice.	
3.	Preluarea a unor pasaje (piese de creație de tip text) dintr-o operă autentică publicată anterior, prin parafrază, fără precizarea întinderii și menționarea provenienței și însușirea acestora într-o lucrare ulterioară celei autentice.	
4.	Preluarea identică a unor figuri (piese de creație de tip grafic) dintr-o operă autentică publicată, fără menționarea provenienței și însușirea acestora într-o lucrare ulterioară celei autentice.	✓
5.	Preluarea identică a unor tabele (piese de creație de tip structură de informație) dintr-o operă autentică publicată, fără menționarea provenienței și însușirea acestora într-o lucrare ulterioară celei autentice.	
6.	Republicarea unei opere anterioare publicate, prin includerea unui nou autor sau de noi autori fără contribuție explicită în lista de autori	✓
7.	Republicarea unei opere anterioare publicate, prin excluderea unui autor sau a unor autori din lista inițială de autori.	✓
8.	Preluarea identică de pasaje (piese de creație) dintr-o operă autentică publicată, fără precizarea întinderii și menționarea provenienței, fără nici o intervenție personală care să justifice exemplificarea sau critica prin aportul creator al autorului care preia și însușirea acestora într-o lucrare ulterioară celei autentice.	✓
9.	Preluarea identică de figuri sau reprezentări grafice (piese de creație de tip grafic) dintr-o operă autentică publicată, fără menționarea provenienței, fără nici o intervenție care să justifice exemplificarea sau critica prin aportul creator al autorului care preia și însușirea acestora într-o lucrare ulterioară celei autentice.	✓
10.	Preluarea identică de tabele (piese de creație de tip structură de informație) dintr-o operă autentică publicată, fără menționarea provenienței, fără nici o intervenție care să justifice exemplificarea sau critica prin aportul creator al autorului care preia și însușirea acestora într-o lucrare ulterioară celei autentice.	
11.	Preluarea identică a unor fragmente de demonstrație sau de deducere a unor relații matematice care nu se justifică în regăsirea unei relații matematice finale necesare aplicării efective dintr-o operă autentică publicată, fără menționarea provenienței, fără nici o intervenție care să justifice exemplificarea sau critica prin aportul creator al autorului care preia și însușirea acestora într-o lucrare ulterioară celei autentice.	
12.	Preluarea identică a textului (piese de creație de tip text) unei lucrări publicate anterior sau simultan, cu același titlu sau cu titlu similar, de un același autor / un același grup de autori în publicații sau edituri diferite.	
13.	Preluarea identică de pasaje (piese de creație de tip text) ale unui cuvânt înainte sau ale unei prefețe care se referă la două opere, diferite, publicate în două momente diferite de timp.	

Notă:

a) Prin „proveniență” se înțelege informația din care se pot identifica cel puțin numele autorului / autorilor, titlul operei, anul apariției.

b) Plagiatul este definit prin textul legii¹.

„...plagiatul – expunerea într-o operă scrisă sau o comunicare orală, inclusiv în format electronic, a unor texte, idei, demonstrații, date, ipoteze, teorii, rezultate ori metode științifice extrase din opere scrise, inclusiv în format electronic, ale altor autori, fără a menționa acest lucru și fără a face trimitere la operele originale...”.

Tehnic, plagiatul are la bază conceptul de **piesă de creație** care²:

„...este un element de comunicare prezentat în formă scrisă, ca text, imagine sau combinat, care posedă un subiect, o organizare sau o construcție logică și de argumentare care presupune niște premise, un raționament și o concluzie. Piesa de creație presupune în mod necesar o formă de exprimare specifică unei persoane. Piesa de creație se poate asocia cu întreaga operă autentică sau cu o parte a acesteia...”

cu care se poate face identificarea operei plagiate sau suspicioase de plagiat³:

„...O operă de creație se găsește în poziția de operă plagiată sau operă suspicioasă de plagiat în raport cu o altă operă considerată autentică dacă:

- i) Cele două opere tratează același subiect sau subiecte înrudite.
- ii) Opera autentică a fost făcută publică anterior operei suspicioase.
- iii) Cele două opere conțin piese de creație identificabile comune care posedă, fiecare în parte, un subiect și o formă de prezentare bine definită.
- iv) Pentru piesele de creație comune, adică prezente în opera autentică și în opera suspicioasă, nu există o menționare explicită a provenienței. Menționarea provenienței se face printr-o citare care permite identificarea piesei de creație preluate din opera autentică.
- v) Simpla menționare a titlului unei opere autentice într-un capitol de bibliografie sau similar acestuia fără delimitarea întinderii preluării nu este de natură să evite punerea în discuție a suspiciunii de plagiat.
- vi) Piesele de creație preluate din opera autentică se utilizează la construcții realizate prin juxtapunere fără ca acestea să fie tratate de autorul operei suspicioase prin poziția sa explicită.
- vii) În opera suspicioasă se identifică un fir sau mai multe fire logice de argumentare și tratare care leagă aceleași premise cu aceleași concluzii ca în opera autentică...”

¹ Legea nr. 206/2004 privind buna conduită în cercetarea științifică, dezvoltarea tehnologică și inovare, publicată în Monitorul Oficial al României, Partea I, nr. 505 din 4 iunie 2004

² ISOC, D. Ghid de acțiune împotriva plagiatului: bună-conduită, prevenire, combatere. Cluj-Napoca: Ecou Transilvan, 2012.

³ ISOC, D. Prevenitor de plagiat. Cluj-Napoca: Ecou Transilvan, 2014.

Different title and authorship than the other 3 papers.

This paper is the first one that was submitted out of the 4 papers. E. Andronescu and S. Jinga are missing.



ScienceDirect

Journal of the European Ceramic Society 27 (2007) 1117–1122

ELSEVIER

www.elsevier.com/locate/jeurceramsoc

Effect of the sintering temperature on the Ba(Zn_{1/3}Ta_{2/3})O₃ dielectric properties

A. Ioachim^{a,*}, M.I. Toacsan^a, M.G. Banciu^a, L. Nedelcu^a, C.A. Dutu^a, M. Feder^a, C. Plapcianu^a, F. Lifei^a, P. Nita^b

^a National Institute of Materials Physics, 077125 Bucharest-Magurele, Romania

^b METAV S.A, 020011 Bucharest, Romania

Available online 12 June 2006

Abstract

Preparation of dielectric materials with optimal properties for wireless applications requires special thermal treatments due to the difficult control of the cationic ordering. The BZT samples prepared by solid-state reaction were sintered at temperatures in the range 1400–1600 °C for 4 h. For compositional, structural and morphological characterization, XRD, SEM and EDX were employed. The order–disorder transition of the BZT material was analyzed. With the increase of the sintering temperature, a long-range order with a 2:1 ratio of Ta and Zn cations on the octahedral positions of the perovskite structure was observed. The dielectric parameters were measured in the microwave range and were correlated with morphological and structural properties. In order to improve the microwave properties, annealing treatment at 1400 °C for 10 h was performed. Sintering temperatures greater than 1550 °C are required for undoped BZT compositions, in order to obtain low microwave loss ($Qf > 100,000$). © 2006 Elsevier Ltd. All rights reserved.

Keywords: Tantalates; Sintering; Microstructure; Dielectric properties; Super-high- Qf

1. Introduction

Ba(Zn_{1/3}Ta_{2/3})O₃ (BZT) is a perovskitic material of the A(B'B'')O₃ type, having ultra high values of the quality factor Q . It has potential for applications in satellite broadcasting at frequencies higher than 10 GHz and as a super-high- Q dielectric resonators (DR) in mobile phone base stations or combiner filter for PCS applications.¹ The BZT ceramics exhibit a dielectric constant of 29, a Qf product of 100,000–150,000 and a low temperature coefficient of resonant frequency (τ_f).

The factors influencing Q values of perovskites Ba(M_{1/3}²⁺Ta_{2/3}⁵⁺)O₃ (M=Mg, Zn) have been considered to be long-range ordering (LRO) of cations, zinc oxide evaporation, point defects and stabilization of microdomain boundaries.^{2,3} This explained the high- Q values from the point of view of the lattice vibrations of its hexagonal superstructure. Sagala and Nambu⁴ calculated the dielectric loss tangent at microwave frequencies from the equation of ion motions which was a function of B-site ordering. Gallasso and coworkers⁵ concluded that the B-site ordering increased as the difference

in charge and size between B' and B'' atoms increased. The ordering of complex perovskite BZT is important because the 1/3 < 1 1 > (1:2) ordering is believed to be closely related to the high- Q property of BZT. There is a strong correlation between the cation ordering, domain growth, zinc loss and sintering parameters. In this paper we report the synthesis of a BZT material, its structural and morphologic characteristics as well as its microwave dielectric properties.

2. Experimental

Ceramics with molar formula Ba(Zn_{1/3}Ta_{2/3})O₃ were prepared by solid-state reaction. The starting materials were BaCO₃, ZnO and Ta₂O₅. Stoichiometric quantities were weighted, ground, homogenized and milled in an agate mill in water for 2 h. The powders were calcined at $T=925$ °C for 2 h. Then the powders were milled for 2 h and calcined at 1000 °C for 2 h. The calcined powders were mixed with 1% polyvinylalcohol (PVA) and dried at $T=80$ °C were pressed into cylindrical samples of 12 mm diameter and 10 mm height. The pellets were slowly dried at 80 °C in order to eliminate the PVA. The third calcination was carried out at $T=1150$ °C in air for 2.5 h.

* Corresponding author. Tel.: +40 21 4930173/123; fax: +40 21 4930267.
E-mail address: ioachim@infim.ro (A. Ioachim).

In the other articles it is 4400 Kg/m3 ... same quantity, written differently. The same goes for 7.92 g/cm3 below.

The TSF paper reads "the (111) plane", whereas here it reads "the plane normal to (111)", although they both refer to the same experiment and same numerical values.

The density of green ceramics was $\rho = 4.4 \text{ g/cm}^3$. The sintering treatment was performed in air for 4 h at six temperature values: 1400, 1450, 1500, 1525, 1550 and 1600 °C. In order to increase the dielectric properties, especially the quality factor Q , the samples were treated supplementary for 10 h at 1400 °C. The pellets were polished to remove the superficial zone, which is porous and poor in Zn, in order to obtain correct values of the microwave dielectric parameters.

The relative bulk density of sintered cylinders was measured by the Archimedes method. Morphological, structural and compositional analyses were performed on six sets of samples by X-ray diffraction (XRD) analysis, and electron microscopy (SEM, EDX). The patterns were recorded in a 2θ range from 20° to 90° on a Seifert Debye Flex 2002 diffractometer into the $2\theta - \theta$ mode. Measurements were performed at room temperature using Cu $K\alpha$ radiation, Ni filter and a detector scan speed of 7°/min. In order to obtain information on cation ordering state and unit cell distortion a detector scan speed of 5°/min was used.

The dielectric parameters, i.e. the dielectric constant ϵ , the quality factor Q and the loss tangent $\tan \delta$ were measured in the microwave range by Hakki-Coleman method. A computer aided measurement system containing a HP 8757 C scalar network analyzer and a HP 8350 B sweep oscillator was employed.

stoichiometric ratio, in the sequence Zn-Ta-Ta-Zn-Ta-Ta... The resulting symmetry, due to the (1 1 1) type plane stacking and accompanying small oxygen displacement strongly depends on processing parameters. So, the ordering of Zn and Ta depends on firing temperature and of the sintering time. The BZT sintered at lower temperatures ($T_s < 1300^\circ\text{C}$) exhibits a pseudo-cubic perovskite type structure where Zn and Ta are in disorder. At higher sintering temperatures ($T_s > 1300^\circ\text{C}$) BZT has a hexagonal perovskite type structure, with Zn and Ta showing 1:2 order in the B site. The order of Zn and Ta expands the original perovskite unit cell along the $\langle 111 \rangle$ direction and contracts the unit cell in the plane normal to $\langle 111 \rangle$. Consequently, cla has a value greater than $\sqrt{3/2} \approx 1.2247$ and the unit cell is distorted.

The increase of cation ordering on B site in BZT compounds creates a superlattice with a hexagonal structure. The degree of long-range-structural order (LRO) can be measured by X-ray methods and it can be expressed as the ratio between the intensity of the super structure reflection and that of a basic unit cell reflection. The X-ray diffraction patterns for BZT compound, sintered at six sintering temperatures, using Cu $K\alpha$ radiation are given in Fig. 1. The X-ray patterns confirm the formation of the hexagonal structure, which is the majority phase. For the BZT compounds sintered at $T_s = 1500$ and 1525°C the patterns reveal the presence of secondary phases $\text{Ba}_7\text{Ta}_6\text{O}_{22}$, Ba_8ZnTa_4 and BaO , which disappear at higher sintering temperatures. The order structure was examined in the XRD patterns by observing

3. Results and discussion

Figure instead of table in ROMJIST, IEEE & TSF.

3.1. Bulk density

The bulk density of the fired BZT ceramics was measured after grinding and polishing. The temperature dependence of densification after 4 h sintering in air is shown in Table 1. BZT ceramics sintered between 1400 and 1600 °C were well sintered.

The X-ray density of $\text{Ba}(\text{Zn}_{1/3}\text{Ta}_{2/3})\text{O}_3$ compound with stoichiometric composition was considered as $\rho_t = 7.92 \text{ g/cm}^3$. The most dense ceramic presents a porosity value of $P = 10\%$. An abnormal grain growth together with an accentuated ZnO evaporation occurred above 1525 °C, so the bulk density slightly decreased.

3.2. X-ray diffraction analysis

The crystal structure of $\text{Ba}(\text{Zn}_{1/3}\text{Ta}_{2/3})\text{O}_3$ is of a classic ordered perovskite with two transition metals (B' and B'') on the octahedral site. The B' and B'' ions occur on alternating (1 1 1) planes in a 1:2 ratio. Each (1 1 1) plane contains only one type of small oxygen octahedron, and the planes are ordered in the 1:2

Table 1 Density vs. sintering temperature for BZT samples sintered in air for 4 h

Sintering temperature (°C)	Bulk density ρ_0 (10^3 kg/m^3)	Absorption capacity (%)	Porosity P (%)
1400	5.37	5.3	32.1
1450	6.22	2	21.4
1500	7.10	0.9	10.3
1525	6.90	0.6	12.8
1550	6.93	0.7	12.5
1600	7.04	0.6	11.1

Identical values to Fig 1 in ROMJIST, IEEE and TSF.

This part of the figure is the same as in the other 3 papers.

This part of the figure is missing from the other 3 papers, even though they were pub'd 1-2 years

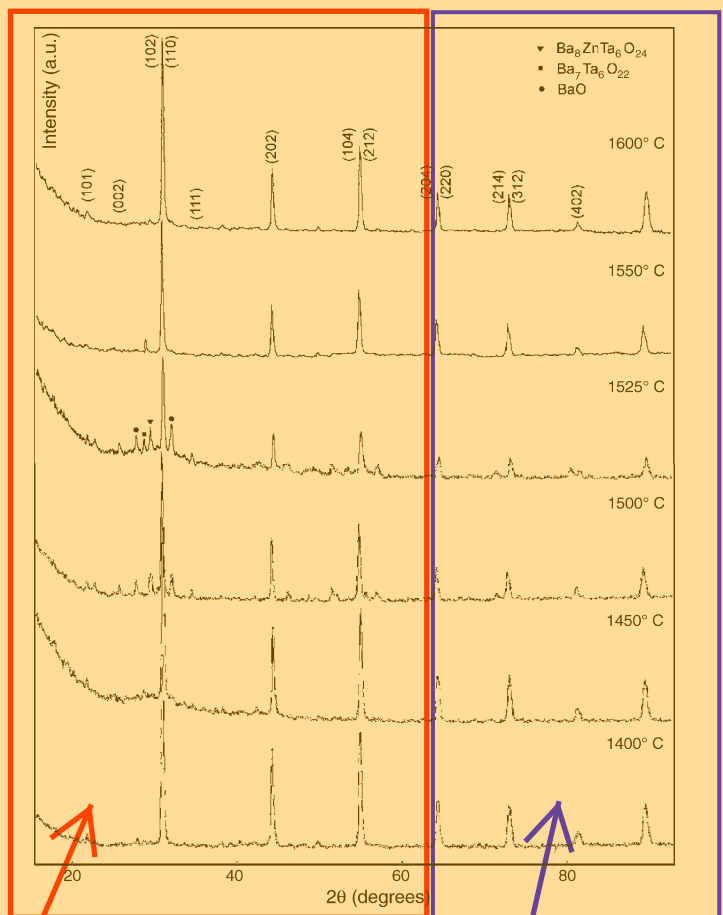


Fig. 1. XRD patterns of $\text{Ba}(\text{Zn}_{1/3}\text{Ta}_{2/3})\text{O}_3$ system vs. sintering temperature.

In the TSF paper, these values are the same but are expressed in nm rather than Angstroms.

the reflections due to Zn and Ta order (superstructure reflection) and the line split, i.e. the c/a differs of $\sqrt{3}/2$. The former shows the amount of Zn and Ta ordering and the latter shows the lattice distortion by Zn and Ta ordering. In the superstructure lines, the reflections whose index $(2h + k + l)/3$ does not equal the integer, are caused by the Zn and Ta. Therefore, a change in intensity of the superstructure reflection corresponds to the amount of Zn and Ta order. The (100) reflection has the strongest intensity among the superstructures lines. Fig. 1 shows the increase in intensity of (100) reflection versus sintering temperature for 4 h treatments time. LRO gradually increase up to 1600 °C.

Lattice distortion caused by Zn and Ta ordering can be evaluated by the split of the (422) and (226) reflections. If no distortion occurs, then the (422) and the (226) reflections are not separated. Fig. 2 shows the profile change of (422) and (226) reflections versus sintering temperature. Diffraction patterns show that the ceramics fired up to $T_s = 1500$ °C consist of half distorted and half non-distorted structure. In ceramics fired from 1525 to 1600 °C, a split of (422) and (226) reflections can be observed.

The perfectly ordered structure is produced by the following process:

1. A perovskite-type structure is formed, but Zn and Ta are in disorder.
2. Zn and Ta are partially in order.
3. Zn and Ta are completely in order and the lattice is distorted.

A supplementary distortion can be produced by the ZnO loss. At high sintering temperatures, ZnO evaporates. The Zn^{2+} ions on B'-site are partially replaced by Ba^{2+} , which have a much larger ionic size 1.61 Å comparatively to 0.74 Å for Zn. This substitution creates a supplementary unit cell distortion,⁷ even when the LRO is saturated and leads to an increase of Q .

3.3. Analysis of microstructure and composition

The microstructure of BZT ceramics sintered in air at 1550 °C/4 h was investigated by using SEM. The images are presented in Figs. 3–6. The BZT samples sintered at $T_s > 1500$ °C present grains with concentric ordered shells. BZT sample has a porous structure due to ZnO evaporation during the sintering process. In Fig. 3 is presented a micrograph of the sample periphery. The SEM image reveals an extended porosity, with pore size in the range (10–30) μm, inter-aggregates. Smaller pores, between 3 and 5 μm, are located between grains. Submicron pores appear only on the grain surface. The large grains of an octahedron shape, well faceted and with sizes in the range (10–20) μm are present in all the samples. Micron grains are located on the grain boundaries or on the grain surfaces.

The SEM image of the central zone of BZT sample sintered at 1550 °C for 4 h is shown in Fig. 4. In this case the porous structure is reduced comparatively with the spherical zone. The large pores disappear. There are inter-aggregates pores with sizes between 5 and 10 μm. Moreover, there are smaller pores ones located between three and four grains with sizes (1–3) μm. The micrograph presents a bimodal distribution of

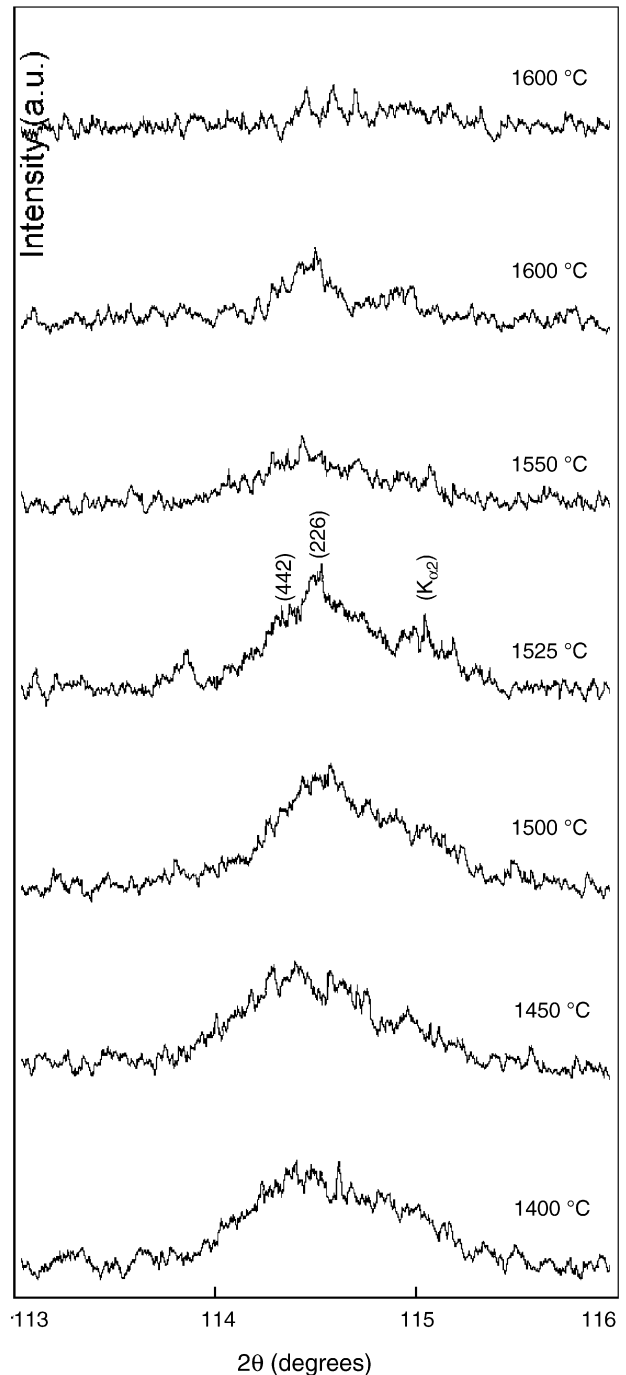


Fig. 2. The (226) and (422) reflection profiles of BZT ceramics vs. sintering temperature.

grains size. Well faceted, polyhedral grains with dimensions in the range (20–40) μm are present with smooth surfaces and edges. It appears that the dislocations climbed and dissociated (region a in Fig. 5) when the material was partially in ordered state and that the dislocation configurations became frozen when disorder set in during granular growth. In most cases, the less-ordered area was associated with at least one dislocation, weak 1:1 order, surrounded by areas with 1:2 order. Few micron grains (1–3) μm, are located on the smooth layer grains surfaces with a cubic-deformed shape (region b in Fig. 5). Other micron grains

Even though these pictures look different than in the other 3 papers, the numerical values and graphs on the next page are the same in all 4 papers.

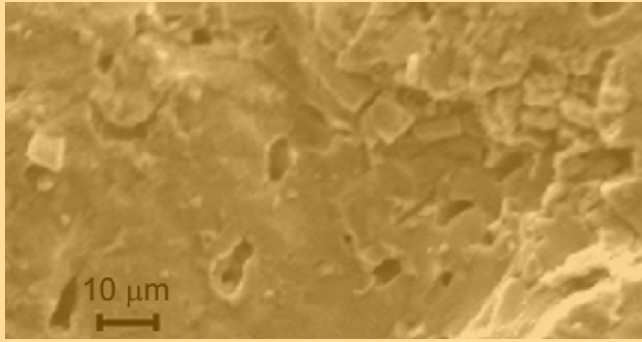


Fig. 3. Micrograph of the periphery of the BZT sample sintered 1550 °C/4 h.

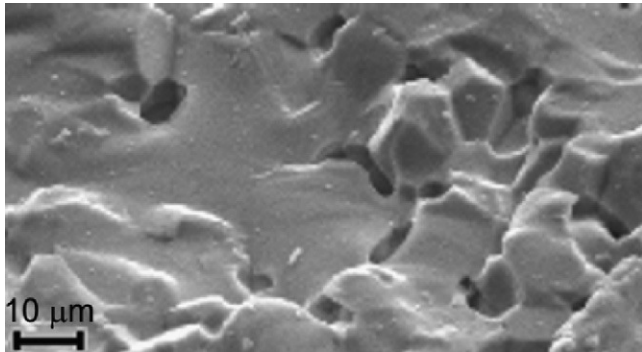


Fig. 4. SEM micrograph of BZT sintered in air for 4 h at 1550 °C—core zone.

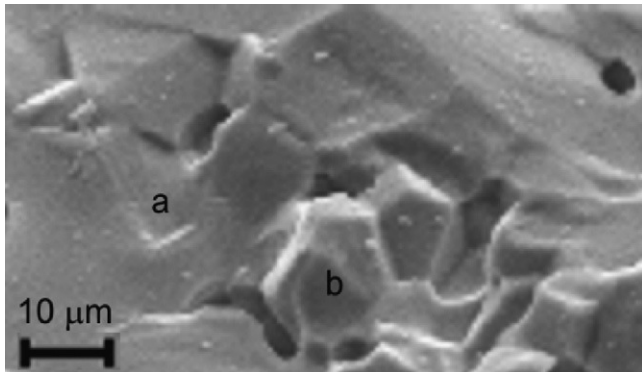


Fig. 5. Detail of SEM image from Fig. 4: (a) dislocations climbed and dissociated in a BZT grain; (b) small cubic-micron grains located on the surface of large octahedral well faceted ones.

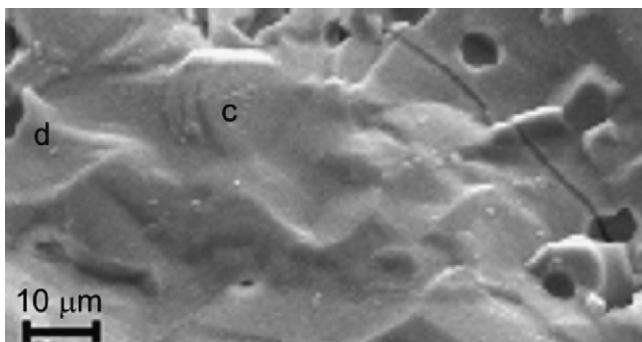


Fig. 6. Micrograph of 1:2 ordered compound BZT: (c) region containing very large domains of order; (d) very large grains with curved edges.

Table 2

EDX data: atomic concentration percents of basic elements of BZT specimen sintered for 4 h at 1550 °C in air

Ba (%)	Ta (%)	Zn (%)	Position on the disk
57.18	41.97	0.86	Outer zone
53.53	45.43	1.04	Inner zone

with spherical shape are agglomerate in aggregates of (6–8) μm near the boundaries of larger grains.

The micrographs reveal the presence of few very large grains ($d > 50 \mu\text{m}$), with curved edges, corresponding to the abnormal granular growth (region d in Fig. 6). The abnormal granular growth together with the ZnO evaporation can explain the bulk density decrease of BZT specimens sintered at $T_s > 1500 \text{ }^\circ\text{C}$.

We used microanalysis (EDX) in an attempt to examine whether a composition trend such as a “paucity” of the B' element could explain the correlation between microstructure, long-range ordering and dielectric properties. The inner and outer zone compositions are presented in Table 2. The Zn atomic concentration indicates a sub-stoichiometric composition, accentuated at the sample periphery where the ZnO evaporation is more possible. On the other hand, the experimental data indicate a variation of Ba^{2+} content with higher concentration at the sample boundary. In this case, Ba^{2+} can enter on the free Zn-octahedron sites, producing a supplementary deformation of the unit cell.

3.4. Microwave measurements

Microwave measurements on dielectric constant and loss tangent were performed on the BZT 1–5 samples. The data obtained revealed a determinant influence of the sintering temperature as well as of the annealing on the complex dielectric constant. The increase of the dielectric constant with the increase of the sintering temperature can be observed in Table 3. This can be considered as an effect of the reduced porosity resulting in a better densification at high sintering temperatures, as can be seen in Table 1.

The loss tangent exhibits values around 2×10^{-4} for samples sintered at 1400 and 1450 °C. The dielectric loss tangent increases to 7×10^{-4} with the sintering temperature increases to 1500–1550 °C, then it decreases 2×10^{-4} for samples sintered at 1600 °C. This variation could be related with the Zn and Ta cation ordering process and with the secondary phases, which appear for sintering temperatures between 1450 and 1525 °C as shown in Fig. 1. For temperatures higher than 1550 °C these phases disappear and, consequently, the dielectric loss became lower.

The additional thermal treatment at 1400 °C for 10 h for all samples resulted in the reduction of the BZT dielectric loss as can be seen in Table 4 and Fig. 7. The quality factor Q of annealed samples is higher than for samples without thermal treatment, especially for samples sintered beyond 1550 °C. The quality factors Q of the annealed BZT4 and BZT5 samples take values up to 18,000 and the dielectric permittivity is around 31 as shown in Fig. 8 and Table 4.

The numerical values from these tables are also found in the three graphs below, which are the same in all 4 papers.

Table 3
Dielectric parameters of BZT ceramics vs. sintering temperature

Sample	Sintering temperature (°C)	Resonance frequency f (GHz)	Dielectric permittivity ϵ_r	Dielectric losses $tg\delta (\times 10^{-4})$	Quality factor Q	Product Qf (GHz)
BZT 1	1400	7.18	20.8	1.9	5130	36830
BZT 2	1450	6.66	26.6	1.8	5550	36960
BZT 3	1500	6.33	31.1	7	1230	7790
BZT 4	1525	6.29	32	6.6	1230	7740
BZT 5	1600	6.23	34.4	2.1	4600	28660

Table 4
Dielectric parameters of BZT ceramics annealed at 1400 °C/10h vs. sintering temperature

Sample	Sintering temperature (°C)	Resonance frequency f (GHz)	Dielectric permittivity ϵ_r	Dielectric losses $tg\delta (\times 10^{-4})$	Quality factor Q	Product Qf (GHz)
BZT 1	1400	7.73	20.7	2.6	3910	30220
BZT 2	1450	7.12	26.4	1.3	7710	54800
BZT 3	1500	6.75	30.7	1.1	9090	61360
BZT 4	1525	6.73	31.6	0.66	15210	102360
BZT 5	1600	7.51	31.8	0.55	18220	136830

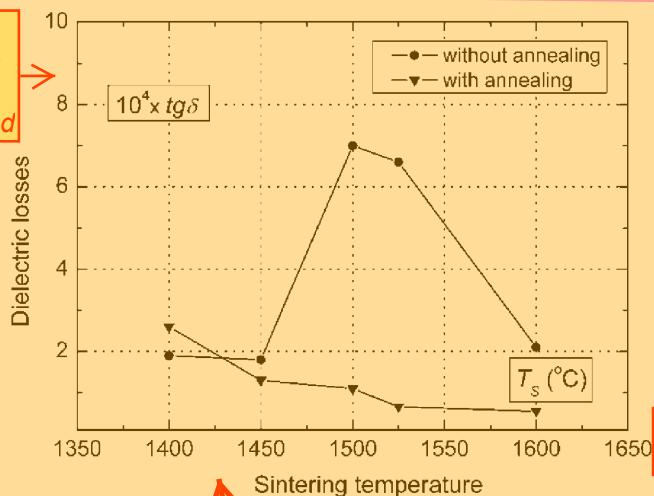


Fig. 7. Modification of dielectric losses curve vs. sintering temperature for BZT ceramics without and with annealing treatment at 1400 °C/10h.

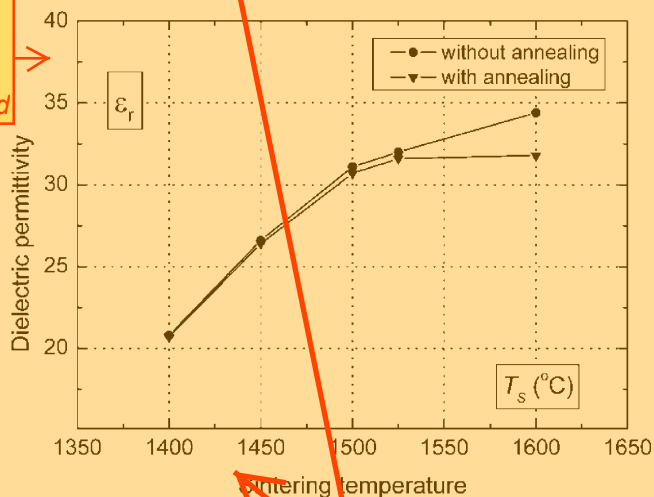


Fig. 8. Modification of dielectric permittivity curve vs. sintering temperature for BZT ceramics without and with annealing treatment at 1400 °C/10h.

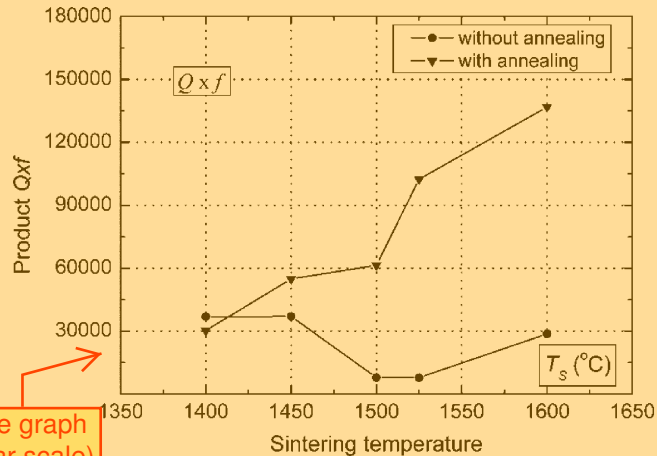


Fig. 9. Modification of the product Qf curve vs. sintering temperature for BZT ceramics without and with annealing treatment at 1400 °C/10h.

The product Qf between the quality factor Q and the measurement frequency f also increases with the sintering temperature for annealed samples as shown in Fig. 9. This could indicate the necessity of an increased sintering time.

4. Conclusions

$Ba(Zn_{1/3}Ta_{2/3})O_3$ ceramics with low loss in microwave domain were obtained by solid-state reaction. The investigations on dielectric properties revealed that the increase of sintering temperature decrease the dielectric loss especially when an annealing of 10 h at 1400 °C is performed.

Qf product strongly depends on the BZT crystalline structure: the unit cell distortion and cationic order. Dielectric loss decreases with the increase of ordering degree in the structure and with the disappearance of secondary phases. Lowest loss is obtained for a Zn and Ta completely ordered BZT ceramic with a strongly distorted unit cell. Porosity has small effect on dielectric loss of BZT material.

In the other 3 papers, the above two graphs have swapped the curves. They are however identical in all 4 papers.

Well-sintered and annealed BZT samples exhibit a dielectric constant around 31 and a Qf product up to 130,000. Super-high quality factor of BZT materials recommend them for microwave and millimeter wave such applications as resonators and filters for wireless communication systems.

Acknowledgement

This work was supported by Ministry of Education and Research under contract nr.: 09N/505.2003

References

1. Kawashima, S., Influence of ZnO evaporation on microwave dielectric loss and sinterability of $\text{Ba}(\text{Zn}_{1/3}\text{Ta}_{2/3})\text{O}_3$ ceramics. *Am. Ceram. Soc. Bull.*, 1993, **72**(5), 120–126.

Different grant than the other 3 papers.

2. Desu, S. and O'Bryan, H. M., Microwave loss quality of $\text{Ba}(\text{Zn}_{1/3}\text{Ta}_{2/3})\text{O}_3$ ceramics. *J. Am. Ceram. Soc.*, 1985, **68**(10), 546–551.
3. Tamura, H. et al., Lattice vibrations of $\text{Ba}(\text{Zn}_{1/3}\text{Ta}_{2/3})\text{O}_3$ crystal with ordered perovskite structure. *Jpn. J. Appl. Phys.*, 1986, **25**(6), 787–791.
4. Sagala, D. S. and Nambu, Microscopic calculation of dielectric loss at microwave frequencies for complex perovskite $\text{Ba}(\text{Zn}_{1/3}\text{Ta}_{2/3})\text{O}_3$. *J. Am. Ceram. Soc.*, 1992, **75**(9), 2573–2575.
5. Gallasso, F. and Pyle, J., Ordering in compounds of the $\text{A}(\text{B}'_{1/3}\text{Ta}_{2/3})\text{O}_3$ type. *Inorg. Chem.*, 1983, **2**(3), 482–484.
6. Roulland, F. et al., Influence of both milling condition and lithium salt addition on the sinterability of $\text{Ba}(\text{Zn}_{1/3}\text{Ta}_{2/3})\text{O}_3$. *Mater. Sci. Eng. B*, 2003, **104**, 156–162.
7. Ioachim, A. et al., Synthesis and dielectric properties of $\text{Ba}(\text{Zn}_{1/3}\text{Ta}_{2/3})\text{O}_3$. In *The IXth Int. Conf. "Sci. and Ed."*, 2004.